

## Refined 1.2 Å crystal structure of the complex formed between subtilisin Carlsberg and the inhibitor eglin c. Molecular structure of eglin and its detailed interaction with subtilisin

Wolfram Bode, Evangelos Papamokos, Djordje Musil, Ursula Seemueller<sup>1</sup> and Hans Fritz<sup>1</sup>

Max-Planck-Institut für Biochemie, D-8033 Martinsried/München, and <sup>1</sup>Abteilung Klinische Chemie und Klinische Biochemie, Universitaet München, D-8000 München 2, FRG

Communicated by R. Huber

The crystal structure of the complex formed between eglin c, an elastase inhibitor from the medical leech, and subtilisin Carlsberg has been determined at 1.2 Å resolution by a combination of Patterson search methods and isomorphous replacement techniques. The structure has been refined to a crystallographic *R*-value of 0.18 (8–1.2 Å). Eglin consists of a four-stranded  $\beta$ -sheet with an  $\alpha$ -helical segment and the protease-binding loop fixed on opposite sides. This loop, which contains the reactive site Leu45I–Asp46I, is mainly held in its conformation by unique electrostatic/hydrogen bond interactions of Thr44I and Asp46I with the side chains of Arg53I and Arg51I which protrude from the hydrophobic core of the molecule. The conformation around the reactive site is similar to that found in other proteinase inhibitors. The nine residues of the binding loop Gly40I–Arg48I are involved in direct contacts with subtilisin. In this interaction, eglin segment Pro42I–Thr44I forms a three-stranded anti-parallel  $\beta$ -sheet with subtilisin segments Gly100–Gly102 and Ser125–Gly127. The reactive site peptide bond of eglin is intact, and Ser221 OG of the enzyme is 2.81 Å apart from the carbonyl carbon.

**Key words:** complex/crystal structure/eglin/inhibitor/subtilisin

### Introduction

Eglins are small protein inhibitors isolated from the leech *Hirudo medicinalis* (Seemueller *et al.*, 1977). They effectively inhibit chymotrypsin and subtilisin as well as the granulocytic proteinases elastase and cathepsin G. They consist of a single polypeptide chain of 70 amino acid residues (Seemueller *et al.*, 1980) and show strong sequence homology with the potato inhibitor 1 family (Svendsen *et al.*, 1982). Eglin b and c differ by a single amino acid exchange at position 35 (His versus Tyr; Chang *et al.*, 1985). In spite of lack of any disulfide bridges, eglin is very resistant against heat or acid denaturation. Its specific inhibitory spectrum makes eglin a valuable tool as an anti-inflammatory agent. Synthetic eglin genes have recently been synthesized and expressed in *Escherichia coli* (Rink *et al.*, 1984).

Subtilisins form a distinct family of serine proteinases of bacterial origin. Best characterized are subtilisin BPN' (Novo) and subtilisin Carlsberg. The sequence of the 274 amino acid residues of subtilisin Carlsberg has been determined (Smith *et al.*, 1968). The crystal structures of subtilisin BPN' (Novo) (Wright *et al.*, 1969; Drenth *et al.*, 1972) as well as its complex formed with the *Streptomyces* subtilisin inhibitor (SSI; Hirono *et al.*, 1984) are known. Compared with subtilisin BPN' there are 84 residue

differences and one deletion in subtilisin Carlsberg (Markland and Smith, 1971).

We have been able to crystallize several eglin complexes formed with granulocytic elastase and different subtilisin species. Previously we have communicated the crystal data of the complex formed between natural eglin c from leech and subtilisin Carlsberg (Bode and Schirmer, 1985). Very recently preliminary data about the main chain fold of a similar complex formed with recombinant eglin have been presented (McPhalen *et al.*, 1985). We have independently determined and now completely refined the eglin–subtilisin complex. In this paper we describe the complete high resolution structure of natural eglin c and its detailed interaction with subtilisin Carlsberg. The course of the structure analysis and the subtilisin structure will be described elsewhere.

### Results

#### Conformation of eglin

The subtilisin–eglin complex has a mushroom-like shape with the eglin as the stem. Eglin [Figure 1, produced with a program written by Lesk and Hardman (1982)] has the shape of a wedge, with its pointed edge formed by the protease-binding loop Pro42I–Arg48I. Besides this wide loop containing the scissile bond Leu45I–Asp46I, the peptide chain is organized (classified according to main-chain conformation, compare with Figures 1 and 2) in four  $\beta$ -strands (Lys8I–Phe10I; Asn33I–Leu37I; Arg51I–Tyr56I; His65I–Gly70I), in a straight 3.6<sub>13</sub>  $\alpha$ -helical segment (Val18I–Tyr29I) of 3.4 turns (including Thr17I), and (according to its hydrogen bond pattern) in an approximate 3<sub>10</sub>-helix (Phe10I–Val14I) of 1.5 turns. These elements of periodic regular structure are connected by tight turns of type I (Tyr29I–Tyr32I and Arg48I–Arg51I) and type II (Val13I–Lys16I, Pro38I–Ser41I and Asn57I–Thr60I). All favourable intramolecular hydrogen bonds selected according to stereochemical criteria are shown in Figure 2 and listed in Table I. Strands Asn33I–Glu39I and Asn50I–Tyr56I form a regular parallel  $\beta$ -pleated sheet with a strong right-handed twist (if viewed along the strands). The topological connectivity of both strands can be described as a right-handed cross-over connection of type a+1x (Richardson, 1981) or  $\beta c\beta$ . Furthermore, the carboxy-terminal segment runs anti-parallel to strand Asn50I–Asn57I. Both segments are connected only by inter main-chain hydrogen bonds at both ends of the sheet (Asn57I N. . .Val62I O and Gly70I N. . .Arg51I O) and by many side-chain interactions. The carboxy-terminal segment Asn61I–Val69I, in turn, runs anti-parallel to the amino-terminal segment Lys8I–Val18I. The arrangement of  $\beta$ -strands can be described as  $-3x, +1x, +1$  (Richardson, 1981). Thus the gross structure of eglin can be characterized as an irregular four-stranded  $\beta$ -pleated sheet twisted to form a bowl filled at its concave side by the  $\alpha$ -helical segment and bridged at its convex side by the wide eglin loop.

The amino-terminal segment of eglin is defined by appropriate electron density only from Lys8I onwards (including its side-chain which does not specifically interact). There is no density for

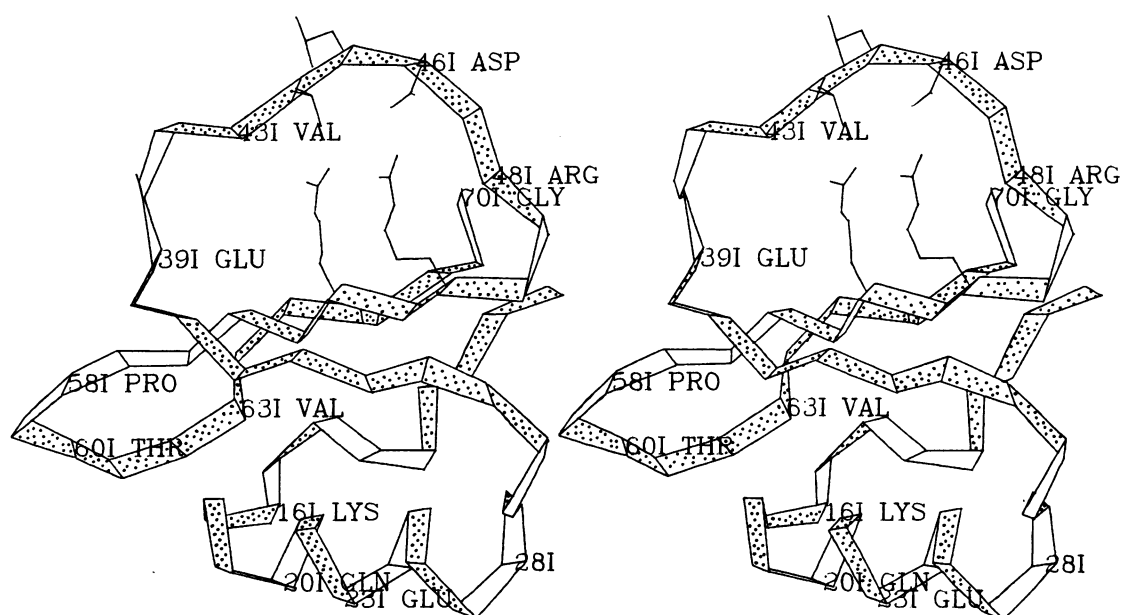


**Fig. 1.** Ribbon diagram of the eglin polypeptide chain, with creases at each  $\alpha$ -carbon position. Only the side chains of reactive site residues Thr44I, Leu45I and Asp46I and those of Arg51I and Arg53I are fully shown.

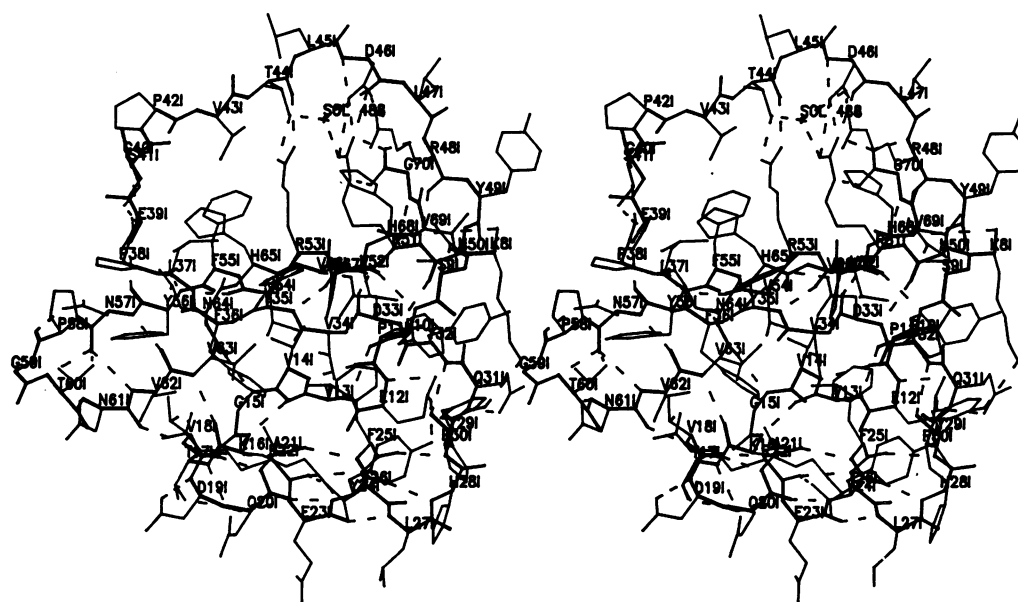


**Fig. 2.** Complete structure of the eglin c molecule. Main chain atoms are connected by thick lines and probable hydrogen bonds are shown by dashed lines.

preceding residues. In the optimal hydrogen bond distance of Lys8I N are two well-separated density lobes representing solvent molecules. Disc electrophoreses of dissolved crystalline material and amino-terminal sequencing of separated peptides indicate that an acidic (approximately seven residues long) peptide is split from the amino-terminus.

The hydrophobic side chains of residues Phe10I, Val13I, Val18I, Ala21I, Phe25I, Val34I, Phe36I, Leu37I, Val43I, Val52I, Val54I, Phe55I, Tyr56I, Val63I, Pro67I and Val69I are buried in the interior of the eglin molecule and form a hydrophobic core. The interaction of this core with the reactive site loop Pro42I–Arg48I is mediated mainly through the side chains of Arg51I and Arg53I, with additional hydrophobic contacts via Val43I and the interactions made through the carboxy-terminal Gly70I (see Figure 2). The extended side chains of both these arginine residues are aligned parallel and interact specifically with

charged and polar groups on both sides of the scissile peptide bond. The guanidyl group of Arg51I is in hydrogen bond distance from one of the carboxylate oxygens (OD2) of the P1' residue Asp46I forming a salt bridge. It further exploits all its hydrogen bonding capacity by forming hydrogen bonds to Asp46I O and to two bound solvent molecules (OH 488 and OH 492). The guanidyl group is rigidly linked to the terminal carboxylate of Gly70I through a cyclic hydrogen bonding net (Table I) and electrostatic interactions (Figure 2). The side chain of Asp46I is bent and forms a hydrogen bond with its main chain amide nitrogen, which has no other hydrogen bond partner in its surrounding. The guanidyl group of Arg53I, in contrast, interacts strongly with the P2 residue Thr44I by forming hydrogen bonds with its carbonyl and hydroxyl oxygens. It further binds to Ser99 O of subtilisin (see below) and to two solvent molecules.

Of the 77 localized solvent molecules hydrogen-bonded to eg-

Table I. Possible intramolecular hydrogen bonds in eglin c

Main-chain atom 1	Main-chain atom 2	Distance Å
Lys 81 O	N	2.94
Phe 101 O	N	3.07
Pro 111 O	N	3.16
Val 131 O	N	3.19
Lys 161 O	N	2.95
Thr 171 O	N	2.74
Val 181 O	N	2.85
Asp 191 O	N	3.06
Gln 201 O	N	3.01
Ala 211 O	N	3.09
Arg 221 O	N	3.09
Glu 231 O	N	2.94
Tyr 241 O	N	2.96
Phe 251 O	N	2.75
Tyr 291 O	N	3.36
Asp 331 O	N	2.93
Tyr 351 O	N	2.73
Leu 371 O	N	3.19
Pro 381 O	N	3.14
Arg 481 O	N	3.16
Asn 501 O	N	2.91
Arg 511 O	N	2.65
Val 521 O	N	2.88
Val 541 O	N	2.97
Tyr 561 O	N	2.82
Asn 571 O	N	3.17
Asn 571 O	N	3.39
Asn 611 O	N	3.07
Val 621 O	N	2.87
Val 631 O	N	2.82
Pro 671 O	N	3.04
Gly 701 O	N	2.91
Main-chain atom 1	Side-chain atom 2	Distance Å
Arg 221 O	OG1 Thr 261	3.01
Pro 381 O	OG Ser 411	2.72
Thr 441 O	NEH1 Arg 531	2.85
Asp 461 O	NEH2 Arg 511	2.99
Asn 571 O	OG1 Thr 601	3.15
Pro 581 O	ND2 Asn 571	2.83
Gly 701 O1	NEH2 Arg 511	2.86
Gly 701 O2	NE Asn 511	2.80
Glu 121 N	OE1 Glu 121	3.08
Thr 171 N	OE1 Gln 201	3.23
Asp 191 N	OD2 Asp 191	3.31
Gln 201 N	OG1 Thr 171	3.13
Gln 311 N	OE1 Gln 311	2.66
Asp 461 N	OD2 Asp 461	2.96
Asn 611 N	OD2 Asn 611	3.27
Side-chain atom 1	Side-chain atom 2	Distance Å
Lys 81 NZ	OEH Tyr 291	3.45
Glu 121 OE2	OEH Tyr 241	2.58
Asn 331 OD1	OEH Tyr 351	2.74
Thr 441 OG1	NEH2 Arg 531	2.80
Asp 461 OD2	OG1 Thr 441	3.42
Asp 461 OD1	NE Arg 481	2.77
Asp 461 OD1	NEH2 Arg 481	3.09
Asp 461 OD2	NEH1 Arg 511	3.32
Asp 461 OD2	NEH2 Arg 511	2.80

lin, three are favourably arranged to form hydrogen bonds with guanidyl nitrogens of Arg511 and Arg531. One water molecule (Sol488) is tetrahedrally surrounded by four hydrogen bond partners provided by eglin (Thr441 OG1: 2.78 Å; Asp461 OD1 and OD2: 2.98 Å and 2.86 Å; Arg511 NEH1: 3.10 Å) and by subtilisin (Asn62 OD1: 2.86 Å) and seems to be an integral constituent of the eglin structure.

Running parallel to the side chains of Arg511 and Arg531 and protecting the exposed side of the former against the solvent is a third arginine side chain, Arg481. Its guanidyl group also interacts electrostatically and through hydrogen bonds with the carboxylate of Asp461, but is, in addition, involved in hydrogen bond interactions with polar groups of Asn62 and Tyr209 of subtilisin (see below).

### The complex

The 127 direct intermolecular contacts between non-hydrogen atoms of eglin and subtilisin shorter than 4 Å are given in Table II. Of the 14 intermolecular hydrogen bonds included in the total, six are made between main-chain atoms. Of the eglin component, almost exclusively residues of the reactive site loop, from Gly40I to Arg48I, contribute to binding (Figure 3). As shown in Table III its main-chain dihedral angles from P3 up to P2' are very similar to those observed in the pancreatic trypsin inhibitor (PTI), in the turkey ovomucoid third domain (OMTKY3) and in SSI in their complexes with trypsin (Huber *et al.*, 1974), *Streptomyces griseus* protease B (Read *et al.*, 1983) and subtilisin BPN' (Hirono *et al.*, 1984).

The eglin inhibitor segment Pro42I–Leu45I, i.e. the strand on the amino-terminal side of the scissile peptide bond, is the central segment of a twisted, three-stranded (or, including the subtilisin segment around Tyr167, even four-stranded) anti-parallel  $\beta$ -pleated sheet formed together with subtilisin segments Gly100–Gly102 on one side and Ser125–Gly127 on the opposite side (Figure 3). Besides several side-chain interactions these three  $\beta$ -strands are connected by four favourable inter main-chain hydrogen bonds (Val43I N...Gly127 O: 3.02 Å; Gly127 N...Val43I O: 2.92 Å; Gly102 N...Pro42I O: 3.36 Å; Thr44I N...Gly100 O: 2.89 Å). In addition, the phenolic side chain of Tyr 104 contacts Gly40I and Pro42I and through its distal OEH atom is involved in a hydrogen bond with Gly40I O (2.55 Å). The distance between the peptide nitrogen of Leu45I and the carbonyl oxygen of Ser125 O is 3.82 Å, i.e. too long to be considered as a functional hydrogen bond. Ser221 OG is much closer (2.99 Å) and arranged in a favourable position to form a hydrogen bond with Leu45I N. The side chain of P1 residue Leu45I is involved in numerous intermolecular van der Waals contacts with the subtilisin segments 125–127, 152–155 and 220–221 which mainly line the S1 subsite of subtilisin (Figure 3 and Table II). In addition, however, its side chain is in direct van der Waals contact with a few solvent molecules which in turn are further interconnected with one another and with polar groups of the inhibitor and the enzyme. This reflects the relatively shallow shape and unspecific character of the S1 subsite of subtilisin, leading to its well-known low selectivity for P1 residues (see Markland and Smith, 1971).

The 'scissile' peptide bond Leu45I C–Asp46I N is intact and slightly distorted towards a tetrahedral state (as indicated by a deviation of 0.1 Å of the carbonyl carbon out of the plane, defined by the adjacent atoms CA, O and N; the peptide group has a substantial torsion with  $\omega = 161^\circ$ ). The carbonyl carbon is 2.81 Å from Ser221 OG, i.e. closer than a van der Waals

**Table II.** Intermolecular contacts  $<4 \text{ \AA}$  in the eglin c–subtilisin complex

Eglin	Y35I	L376I	G40I	S41I	P42I	V43I	T44I	L45I	D46I	L47I	R48I	R53I
Subtilisin												
T33							1					
N62											8(2)	
H64							9	1	5		2	
L96							1					
S99	3											1(1)
G100						3	5(1)					3
S101		1			3	1						
G102					3(1)							
Y104			3(1)									
I107					2							
S125							1	1				
L126						3		1				
G127					3	5(2)		2				
G128			2	1								
A129			4									
S130			6									
A152								2				
G154								2				
N155								6(1)	3			
F189										3		
Y209											3(1)	
N218									3	3(1)		
G219								2				
T220								3				
S221								11(2)	2			
Total	3	1	15(1)	1	11(1)	12(2)	17(1)	31(3)	13	6(1)	13(3)	4(1)

Possible hydrogen bonds included in the total are given in parentheses.

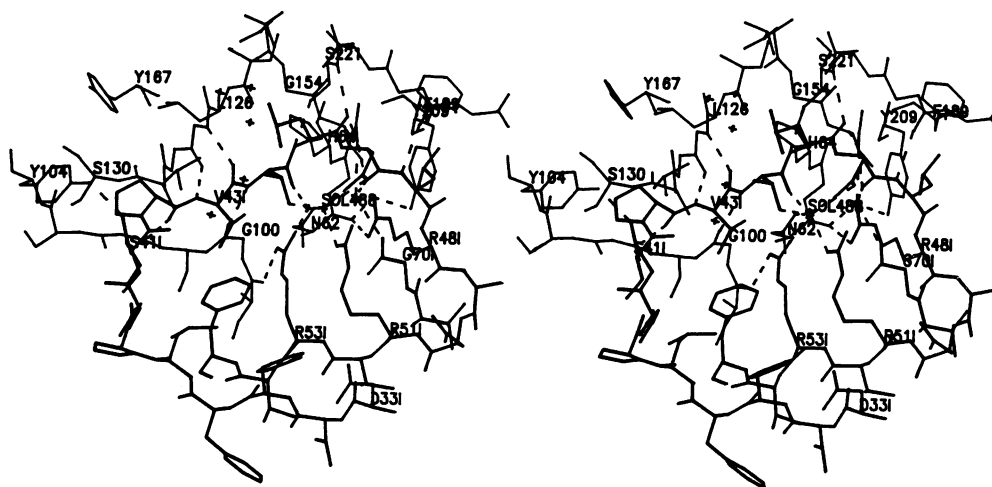


**Fig. 3.** Eglin–subtilisin interface. Eglin segments (Asp33I–Phe55I and Val69I–Gly70I) are given by thick lines, subtilisin segments in contact with eglin by thin lines. Intermolecular hydrogen bonds including those mediated through water molecule Sol488 are shown by dashed lines.

distance. The conformational angle of the side chain of Ser221 is  $-81^\circ$ , i.e. very similar to those observed in the free or complexed serine proteinases of the trypsin-type (Marquart *et al.*, 1983). The OG atom is involved in a straight, favourable hydrogen bond with His64 NE2 (2.73 Å). The carbonyl group of Leu45I points into the oxyanion hole forming bifurcated hydrogen bonds with Asn155 ND2 (2.71 Å) and Ser221 N (3.01 Å). The side chain of Asp46I is shielded from bulk water by the imidazole ring of His64. Leu47I whose hydrophobic side chain is in contact with the benzene ring of Phe189 (Figure 3) forms, through its amide nitrogen, a further inter main-chain

hydrogen bond with Asn218 O (2.85 Å). Finally, Arg48I makes, through its guanidyl group, polar interactions and two hydrogen bonds with Asn62 O (2.96 Å) and Tyr209 OEH (3.35 Å).

Of other parts of the eglin peptide chain, only the side chains of Arg53I (making hydrophobic contacts with main-chain atoms of Ser99–Gly100 and forming a 3.27 Å hydrogen bond Arg53I NEH2...Ser99 O), of Tyr35I (hydrophobic interactions with side-chain atoms of Ser99) and of Leu37I are in direct contact with subtilisin. In addition, a few water molecules (including the ‘integral’ Sol488 OH, shown in Figures 2 and 3) are

Table III. Main-chain conformational angles of eglin c, OMTKY3, SSI and PTI around the reactive site

P-site Inhibitor	P4	P3	P2	P1	P1'	P2'	P3'
Eglin c	-72/138	-141/165	-58/142	-116/47	-98/169	-118/106	-117/109
OMTKY3		-128/146	-69/159	-117/45	-83/153	-99/115	
PTI	76/178	-77/-32	-70/154	-120/49	-94/170	-112/79	-105/120
SSI		-123/141	-52/134	-92/89	-117/169	-120/78	

bridging atoms of both components of the complex.

The chain fold of subtilisin Carlsberg is very similar to that of subtilisin BPN' [according to r.m.s. deviations of 0.775 Å (BPN'; Wright *et al.*, 1969) and 1.03 Å (Novo; Drenth *et al.*, 1972) for all CA atoms excluding residues 52–56]. As already predicted by Kraut (1971) and Markland and Smith (1971) the amino acid replacements and the single deletion do not severely affect the structure. A new structural feature, which has not yet been described, but which should also hold for subtilisin BPN', is the folding of loop segment Leu75–Thr79 around a calcium ion. This calcium is octahedrally liganded by the oxygen atoms of three carbonyls (Leu75, Thr79 and Val81), of two carboxamides (Gln2 and Asn77) and of the carboxylate of Asp41. A detailed description of the subtilisin component will be presented elsewhere.

## Discussion

Chemical and crystallographic evidence suggests that the eglin in the crystalline complex is shortened by seven residues at its amino terminus. In this eglin fragment the amino terminus (Lys8I) and the carboxy terminus (Gly70I) are linked through hydrogen bonds. Residues 1I–7I in intact eglin might be flexible and susceptible towards proteolysis. As a consequence recombinant eglin derivatives to be made in future could probably lack the first seven amino acids without affecting the inhibitory activity. The eglin part observed crystallographically consists mainly of a four-stranded  $\beta$ -sheet strongly twisted to form a bowl with a 3.4 turn  $\alpha$ -helix and an exposed wide binding loop on opposite sides. Its secondary structure roughly agrees with that suggested by prediction methods [e.g. of Chou and Fasman (1974) or Robson (1974)], which, however, suggest a shorter  $\alpha$ -helix.

The interaction of eglin with subtilisin looks quite similar to the interaction observed in the proteinase complexes of the other 'small' serine proteinase inhibitor proteins, obeying the 'standard mechanism' (Laskowski and Kato, 1980). Also in eglin the binding loop is in a conformation which allows it to bind tightly to the cognate enzyme, under formation of a three-stranded (a new feature, not yet observed in other complexes) intermolecular  $\beta$ -sheet. The reactive site bond is only slightly distorted, but remains intact and is, through its carbonyl oxygen, hydrogen bonded in the oxyanion hole. Ser221 OG is 2.8 Å apart from the peptide carbon, but simultaneously forms a favourable hydrogen bond with His64 NE2 (and, in addition, possibly a second one with Leu45I N). Thus this complex is in a conformation similar to that expected for a pre-transition state complex. The relatively rigid and densely packed structure of the complex and the high association rates (Schnebli *et al.*, 1985) observed suggest that the loop structure in the free inhibitor will possess a similar conformation.

Eglin differs, however, from the other 'small' inhibitors in the intramolecular surrounding of the primary binding segment and

in the way this loop is fixed to the central part of the molecule. The arrangement of the main chain outside the binding loop is completely different, thus rendering a nomenclature of 'secondary contact regions' as suggested by Hirono *et al.* (1984) not applicable in this case. The binding loop in eglin is tensed between the two bordering tight turns and held in its favourable exposed conformation mainly by the unique electrostatic and hydrogen bond linkages formed between P2 residue Thr44I and Arg53I on one side and P1' residue Asp46I and Arg51I on the other side of the scissile bond.

Both arginine side chains are characterized by very low temperature factors. This might be a consequence of their contacts with surrounding hydrophobic residues and with the hydrophobic part of Arg48I (see Figure 2), and of the unique interactions made with the carboxy-terminal Gly70I. Also the 'aromatic' behaviour of the guanidyl groups leading in some proteins to a 'stacking' with aromatic side chains (Huber *et al.*, 1974) might favour the adhesion of both arginine side chains. The two clustered positive charges attract strongly the negative dipoles at Thr44I as well as the negative charges of the carboxylate group of Asp46I and of the carboxy terminus at Gly70I. These electrostatic interactions are evidently (in combination with the hydrophobic contacts in their surrounding) as effective in stabilizing the reactive site loop as are the disulfide bridges present in the 'small' Kunitz and Kazal type inhibitors and in SSI where they covalently link the primary binding segment (via P2 or P3) with more internally located segments.

In this way the internal part of the reactive site loop is rigidly clamped in a conformation complementary to the enzyme. The cyclic intra-residue hydrogen bond formed in Asp46I impairs the re-hybridization of this P1' amide nitrogen assumed to be stereochemically required for the formation of the tetrahedral intermediate and to be important in preventing proteolytical cleavage. A similar situation is observed in avian ovomucoid third domain inhibitors where acidic P1' residues forming equivalent intra-residue hydrogen bonds (Papamokos *et al.*, 1982; Read *et al.*, 1983; Bode *et al.*, 1985) are highly conserved (Laskowski *et al.*, 1980). This P1' residue, however, can in other inhibitors like PSTI be replaced by non-carboxylic amino acids.

Up to now it has not been possible to characterize, under non-denaturing conditions, an eglin derivative specifically cleaved at its reactive site. It appears likely that the binding loop in the nicked species is destabilized due to a loss of the delicately balanced interactions with Arg51I and Arg53I. The new ends of the nicked species may refold completely as observed in the 'large' plasma proteinase inhibitors. The structure of modified  $\alpha_1$ -proteinase inhibitor (Loebermann *et al.*, 1984) suggests strongly that in the intact serum inhibitors a similarly looped binding segment occurs.

## Materials and methods

Eglin c of the medical leech was kindly provided by Plantorgan, Bad Zwischenahn. It was isolated as described previously (Seemueller *et al.*, 1977). Its stoichiometric

complex formed with subtilisin Carlsberg (EC3.4.21.14; purchased as subtilisin Nagarse, i.e. BPN', from Serva, Heidelberg) at a 1:1.5 molar ratio of enzyme and inhibitor crystallized in 10% polyethylene glycol (PEG) 6000 (Serva, Heidelberg) buffered with 0.1 M phosphate to pH 6.0 using the hanging-drop vapour-diffusion method. Larger crystals up to  $0.3 \times 0.4 \times 1.0$  mm<sup>3</sup> could be grown by subsequent seeding with whole crystals in fresh protein solutions containing 5% PEG, pH 6.5. Crystals with identical diffraction patterns could also be grown at slightly lower PEG concentrations from recombinant eglin c (kindly provided by Ciba-Geigy, Basel). The crystals are of triclinic space group P1 with cell constants  $a=38.4$  Å,  $b=41.4$  Å,  $c=57.2$  Å,  $\alpha=111.8^\circ$ ,  $\beta=85.8^\circ$ ,  $\gamma=104.7^\circ$ . There is one complex molecule per unit cell (Bode and Schirmer, 1985). The crystals diffract to a Bragg spacing of  $\sim 1.0$  Å.

X-Ray intensity data were collected with CuK $\alpha$  radiation on a rotation camera equipped with a cylindrical film cassette. From five different native crystals, placed in 15% PEG, pH 6.5, 95 000 reflections above the 1  $\sigma$  significance level were collected to 1.2 Å resolution, merged and scaled yielding  $\sim 46$  000 unique reflections (corresponding to 45% of all data expected to 1.2 Å resolution). The final Rmerge [defined as  $\Sigma(I - \langle I \rangle) / \Sigma \langle I \rangle$ ] is 0.092.

The orientation of the subtilisin component in the crystals was determined by Patterson search techniques (Huber, 1965) using observed crystal data to 2.5 Å and the model of subtilisin BPN' (Wright *et al.*, 1969) as deposited at the Brookhaven Data Bank (Bernstein *et al.*, 1977). 2.5 Å Fourier maps calculated with coefficients  $2F_{\text{obs}} - F_{\text{calc}}$  and Sim-weighted model phases allowed the polypeptide chain of the subtilisin component to be traced, but did not show interpretable electron density for the inhibitor (with the exception of the binding segment). After exchanging amino acids and deleting residue 56 of the BPN' model, the crystal structure was refined to an  $R$ -value of 0.26 (6.0–3.0 Å data) using the energy constraint crystallographic refinement EREF (Jack and Levitt, 1978).

To improve the phases, X-ray data from three heavy-atom derivatives (UOAC: 20 mM uranyl acetate in 15% PEG, pH 5; HGAC: 20 mM mercuric acetate in 1 M citrate, pH 8; TRPC: 10 mM *trans*-Pt(NH<sub>3</sub>)<sub>2</sub>Cl<sub>2</sub> in 1 M citrate, pH 8) were collected and their sites refined. The overall figure-of-merit for 6911 phases to 2.5 Å resolution was 0.72. With combined phases obtained from the partial model phases and multiple isomorphous replacement phases, a 2.5 Å Fourier map was calculated which was further improved by solvent flattening. The polypeptide chain of eglin was modelled on a PS300 interactive display system using a modified version of FRODO (Jones, 1978; J.W. Pflugrath, M.A. Saper, J.S. Sack, B.L. Bush and T.A. Jones). The model of the complex was refined in a cyclic manner with repetitive inspection at the display system and of printed difference Fourier maps. The Fourier maps were calculated in the early stages with combined phases and in the final stages with Sim-weighted phases, using data of gradually increasing resolution. At a final stage also individual isotropic  $B$  values were refined. Besides 2443 non-hydrogen protein atoms, 438 solvent molecules (with  $B$ -values  $< 35$  Å<sup>2</sup>) and one bound calcium ion were located in the cell. The final  $R$ -value for all data from 8 Å to 1.2 Å resolution is 0.178.

## Acknowledgements

We gratefully acknowledge the kind gifts of natural and recombinant eglin from Professor E. Fink, Dr R. Maschler and Dr M. Liersch and the continuous help by Drs R. Huber, J. W. Pflugrath, J. Deisenhofer and T. Schirmer. This work has been supported by the Sonderforschungsbereich 207 of the Deutsche Forschungsgemeinschaft.

## References

- Bernstein, F.C., Koetzle, T.F., Williams, G.J.B., Meyer, E.F., Brice, M.D., Rogers, J.R., Kennard, O., Shimanouchi, T. and Tasumi, M. (1977) *J. Mol. Biol.*, **112**, 535–542.
- Bode, W. and Schirmer, T. (1985) *Biol. Chem. Hoppe-Seyler*, **366**, 287–295.
- Bode, W., Epp, O., Huber, R., Laskowski, M., Jr. and Ardelt, W. (1985) *Eur. J. Biochem.*, **147**, 387–395.
- Chang, J.-Y., Knecht, R., Maschler, R. and Seemueller, W. (1985) *Biol. Chem. Hoppe-Seyler*, **366**, 281–286.
- Chou, P.Y. and Fasman, G.D. (1974) *Biochemistry*, **13**, 222–244.
- Drenth, J., Hol, W.G.J., Jansonius, J.N. and Koekoek, R. (1972) *Eur. J. Biochem.*, **26**, 177–181.
- Hirono, S., Akagawa, H., Mitsui, Y. and Iitaka, Y. (1984) *J. Mol. Biol.*, **178**, 389–413.
- Huber, R. (1965) *Acta Crystallogr.*, **A19**, 353–356.
- Huber, R., Kukla, D., Bode, W., Schwager, P., Bartels, K., Deisenhofer, J. and Steigemann, W. (1974) *J. Mol. Biol.*, **89**, 73–101.
- Jack, A. and Levitt, M. (1978) *Acta Crystallogr.*, **A34**, 931–935.
- Jones, A. (1978) *J. Appl. Crystallogr.*, **11**, 268–272.
- Kraut, J. (1971) In *The Enzymes*, 3rd ed., Vol. 3, Boyer, R.D. (ed.), Academic Press, NY and London, pp. 547–560.
- Laskowski, M., Jr. and Kato, I. (1980) *Annu. Rev. Biochem.*, **49**, 593–626.
- Lesk, A.M. and Hardman, K.D. (1982) *Science*, **216**, 539–540.

- Loebermann, H., Tokuko, R., Deisenhofer, J. and Huber, R. (1984) *J. Mol. Biol.*, **177**, 531–556.
- Markland, F.S., Jr. and Smith, E.L. (1971) In Beyer, R.D. (ed.) *The Enzymes*, 3rd ed., Academic Press, NY and London, Vol. 3, pp. 561–608.
- Marquart, M., Walter, J., Deisenhofer, J., Bode, W. and Huber, R. (1983) *Acta Crystallogr.*, **B39**, 480–490.
- McPhalen, C.A., Schnebli, H.-P. and James, M.N.G. (1985) *FEBS Lett.*, **188**, 55–58.
- Papamokos, E., Weber, E., Bode, W., Huber, R., Empie, M.W., Kato, I. and Laskowski, M., Jr. (1982) *J. Mol. Biol.*, **158**, 515–537.
- Read, R.J., Fujinaga, M., Sielecki, A.R. and James, M.N.G. (1983) *Biochemistry*, **22**, 4420–4433.
- Richardson, J.S. (1981) *Adv. Prot. Chem.*, **34**, 167–340.
- Rink, H., Liersch, M., Sieber, P. and Meyer, I. (1984) *Nucleic Acids Res.*, **12**, 6369–6387.
- Robson, B. (1974) *Biochem. J.*, **141**, 853–867.
- Schnebli, H.-P., Seemueller, W., Fritz, H., Maschler, R., Liersch, M., Virca, G.D., Bodmer, J.L., Snider, G.L., Lucey, E.C. and Stone, P.G. (1985) *Eur. J. Resp. Dis.*, **66**, Suppl. 139, 66–70.
- Seemueller, W., Meier, M., Ohlsson, K., Mueller, H.-P. and Fritz, H. (1977) *Hoppe-Seyler's Z. Physiol. Chem.*, **358**, 1105–1117.
- Seemueller, W., Eulitz, M., Fritz, H. and Strobl, A. (1980) *Hoppe-Seyler's Z. Physiol. Chem.*, **361**, 1841–1846.
- Smith, E.L., DeLange, R.J., Evans, W.H., London, M. and Markland, F.S. (1968) *J. Biol. Chem.*, **243**, 2184–2191.
- Svendsen, I., Boisen, S. and Hejgaard, J. (1982) *Carlsberg Res. Commun.*, **47**, 45–53.
- Wright, C.S., Alden, R.A. and Kraut, J. (1969) *Nature*, **221**, 235–242.

Received on 31 December 1985; revised on 24 January 1985